

DEVELOPMENT OF A GUANELLA-TYPE 4:1 IMPEDANCE TRANSFORMER FOR THE FUTURE SIS100 BROADBAND CAVITY SYSTEMS

C. J. Wegmann^{*,1}, H. Klingbeil^{1,2}, R. Balß², M. Frey², U. Laier², S. Orth²

¹Technical University Darmstadt, Darmstadt, Germany

²GSI Helmholtzzentrum für Schwerionenforschung GmbH, Darmstadt, Germany

Abstract

The SIS100 heavy-ion synchrotron under construction at GSI/FAIR will contain a total of 4 broadband cavities for barrier bucket and longitudinal feedback operation. These need to generate non-harmonic gap voltages with relevant spectral components in a range from 100 kHz to 15 MHz. Previous analyses showed that the input capacitance of the tetrode amplifier limits the cavity's upper cutoff frequency. To counteract this effect, the load impedance at the input of the tetrode amplifier shall be reduced from $50\ \Omega$ to $12.5\ \Omega$ at the expense of more driver amplifier power. In this case, achieving an impedance matching to the driver amplifier necessitates the inclusion of a transformer generating a broadband 4:1 impedance transformation over the entire relevant frequency range. A Guanella-type 4:1 ferrite transmission line transformer meeting these requirements was developed, built, and verified by measurement.

INTRODUCTION

The SIS100 heavy-ion synchrotron currently under construction at GSI/FAIR will contain 4 broadband RF cavities for barrier bucket and longitudinal feedback operation [1–3]. These are magnetic alloy / MA-loaded RF cavities (see e.g., Ref. [4]) excited by high-power RF tetrode amplifiers. For the considered types of operation, non-harmonic gap signals with relevant frequency components between 100 kHz and 15 MHz need to be induced.

The tetrode's control grid input, fed by a DC-bias and an RF driver amplifier [5] connected via a LCF12 line [6] of about 100 m length, represents a capacitance of about 800 pF to 1000 pF in parallel to the resistive load. While techniques directly improving the signal quality of the gap voltage are planned – e.g. predistortion [2, 7] – a bottleneck due to impedance mismatching needs to be prevented. One possibility is the inclusion of a transformer allowing for the reduction of the load impedance at the cost of increased driver power as shown in Fig. 1. A secondary-side transmission line with characteristic impedance $Z_L = 25\ \Omega$ and length $l = 1\ \text{m}$ is used to further improve impedance matching. This paper discusses the design of a 4:1 Guanella-type impedance transformer [8] suitable for the considered frequency range and power level (2 kW to 3 kW).

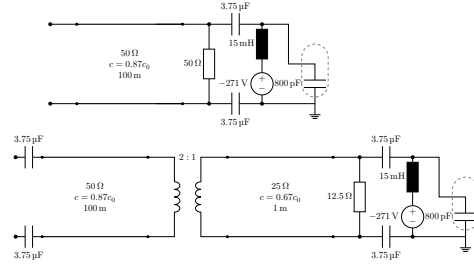


Figure 1: Control grid circuit without (upper diagram) and with 4:1 impedance transformer (lower diagram, voltage ratio 2:1).

BASIC OPERATING PRINCIPLE

Figure 2 shows the circuit diagram of the Guanella-type 4:1 impedance transformer. It features two transmission lines connected in series on the input side and in parallel on the output side [8]. Hence, the input voltage is split over the

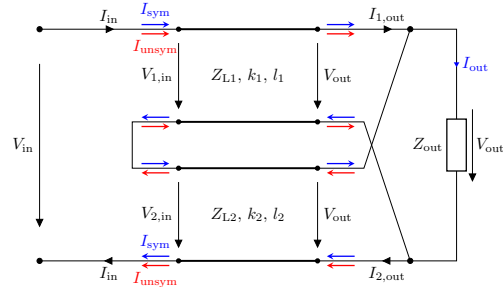


Figure 2: Equivalent circuit of the 4:1 Guanella-type transmission line transformer with symmetrical and unsymmetrical current components [8, 9].

two lines on the primary side while on the secondary side the currents carried by the two lines are added. Since all terminals are connected with each other by DC short circuits, capacitive DC blocks are included in Fig. 1. Assuming exactly equal and opposite (symmetrical) currents carried by the conductors of each line and identical transmission lines with $Z_{L1} = Z_{L2} = Z_L$, $k_1 = k_2 = k$ and $l_1 = l_2 = l$, circuit analysis using standard transmission line equations [10–12] leads to an impedance transformation according to

$$Z_{in} = 4Z_{out} \frac{1 + jt \frac{Z_L}{2Z_{out}}}{1 + jt \frac{2Z_{out}}{Z_L}}, \quad t = \tan(kl). \quad (1)$$

* julien.wegmann@tu-darmstadt.de

With the matching condition $Z_L = 2Z_{\text{out}}$, Eq. (1) yields an ideal impedance transformation

$$Z_{\text{in}} = 4Z_{\text{out}}. \quad (2)$$

Figure 3 shows measurement results of our prototype 4:1 Guanella impedance transformer (in blue) for frequencies from 100 kHz to 20 MHz. For all shown measurements, the reference impedance is $Z_{\text{ref}} = 50 \Omega$. Connections are realized using printed circuit boards, the 25Ω transmission lines by connecting two 50Ω transmission lines in parallel. EN-VIROFLEX_316_D coaxial lines [13] (length $l = 2.8$ m) are used for their power handling capabilities, low bending radius and being free of halogens, as they need to be resistant to radiation in the accelerator tunnel. In the reflection measurement, the transformer is terminated with 4 parallel 50Ω loads. In the transmission measurement, one of the loads is replaced with a VNA port. Hence, only a quarter of the transmitted power is picked up by the VNA reducing S_{21} by half. Since the Guanella transformer acts as a balun [8, 14], an additional balun is necessary to match the balanced transformer output to the unbalanced VNA port.

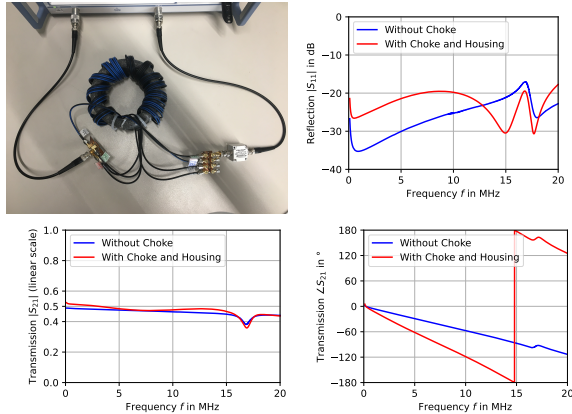


Figure 3: Measurements of prototype Guanella transformers.

The overall system necessitates RF connections to ground (unbalanced voltage) at the driver amplifier and tetrode. Hence, the 4:1 Guanella impedance transformer is supplemented by a 12.5Ω choke coil (or current balun [14, 15]) on its output side, i.e. 4 parallel 50Ω lines wound on a separate core. Thus, Guanella transformer and current balun can be placed in a housing (also important for EMC) without diminishing the performance notably below the target of $|S_{11}| < -20$ dB i.e. less than 1% reflected power (see Fig. 3). The transmission remains almost constant in magnitude and linear in phase with the main difference being the additional delay introduced by the transmission lines of the choke coil.

DESIGN ASPECTS

In practice, the ideal impedance transformation of Eq. (2) is limited by deviations from equal and opposite currents as well as the quarter wave resonance. The upcoming sections discuss these limitations and why the transmission lines need to be wound on a magnetic core.

Lower Operating Limit

For frequencies with wavelengths $\lambda \gg l$, the conductors of the transmission lines can be interpreted as individual inductive windings coupled via the magnetic core [8, 16] leading to the two equivalent circuit diagrams shown in Fig. 4. Two current paths corresponding to the symmetrical and unsymmetrical current through the transmission lines can be identified [8, 9, 17] (see also Fig. 2). Only the symmetrical current transmits power to the load. The unsymmetrical current is counteracted by the windings on the core and, thus, vanishes with increasing frequency (see also [16]). This transition behavior can be seen in the initial drop of reflection in the upper right diagram of Fig. 3. As drawn in Fig. 4, the two lines need to be wound in opposite direction (equivalent to swapping input and output side) so that the magnetizations due to the unsymmetrical currents of both lines are added [17].

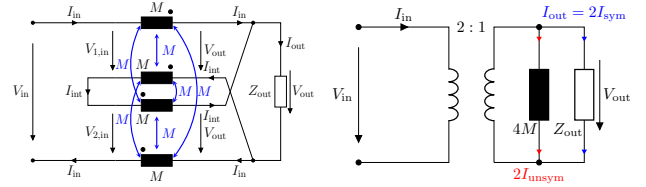


Figure 4: Low-frequency models for the 4:1 Guanella-type impedance transformer [8, 9].

From the right diagram of Fig. 4 with $Z_{\text{ref}} = 4Z_{\text{out}}$, a relation for the lower operating limit can be obtained as

$$f_{-20\text{dB}} = f|_{|S_{11}|=-20\text{dB}} = \frac{1}{2\pi} \frac{\sqrt{99} Z_{\text{out}}}{8 M}. \quad (3)$$

For toroidal cores with cross sections that are small compared to the diameter (and good flux guiding) [18], M can be estimated using

$$M \approx \frac{\mu_r \mu_0 A_e N^2}{l_e}, \quad (4)$$

where A_e is the cross section, l_e the length of the core and N the number of windings. The transformers are build using a stack of two ferrite cores of dimensions 140/106/25 (outer diameter, inner diameter, height in mm) and material 4C65 [19]. This material is used due to its $\mu_r \approx 125$ being almost constant over the considered frequency range. Figure 5 shows how the lower operating limit can be influenced through the number of windings on the core, comparing measurement results from a Guanella transformer prototype with $l = 3.5$ m as well as analytical predictions using Eqs. (3) and (4).

Upper Operating Limit

Considering again the circuit diagram of Fig. 2 but introducing an asymmetry $Z_{L1} = Z_L$, $Z_{L2} = Z_L + \Delta Z_L$ leads to

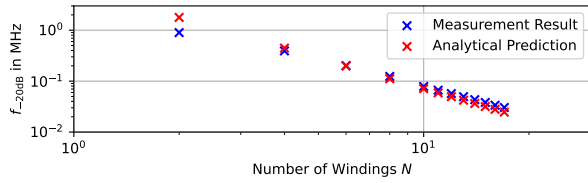


Figure 5: Dependence of the lower operating limit on the number of windings on the magnetic core.

the impedance transformation

$$Z_{\text{in}} = 4Z_{\text{out}} \left[1 + \frac{\Delta Z_L}{2Z_{\text{out}}} \frac{-t^2 \frac{\Delta Z_L}{8Z_{\text{out}}} + jt \left(1 + \frac{\Delta Z_L}{4Z_{\text{out}}} \right)}{\left(1 + \frac{\Delta Z_L}{2Z_{\text{out}}} \right) + jt \left(1 + \frac{\Delta Z_L}{4Z_{\text{out}}} \right)} \right]. \quad (5)$$

Even a small asymmetry can lead to a large mismatch near the quarter-wave resonance where (in the lossless case) $t \rightarrow \infty$. Similar results can be obtained e.g. for asymmetries in kl or asymmetric parasitics. High-power operation near this frequency can damage the transformer. Therefore, shorter transmission lines correspond to a higher upper operating limit (also noted in [17]). Figure 6 visualizes this using two different prototype transformers with lines of length $l = 3.5$ m and $l = 2.8$ m. Note that this implies a trade-off with regard to the lower operating limit as shorter transmission lines means less windings on the core are possible.

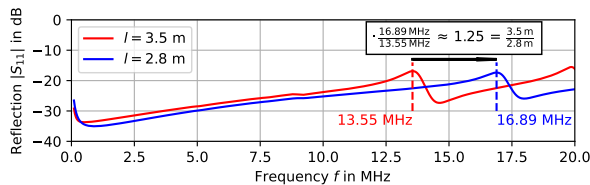


Figure 6: Comparison of impedance transformation for Guanella transformers with lines of different lengths l .

RESULTS

To verify the transformer and circuit design, tests with a prototype setup representing the lower diagram in Fig. 1 were performed (only exception: primary side DC block was not used). Measurement setup and results are shown in Fig. 7. Comparison to simple simulations of the circuits in Fig. 1 shows that the achieved impedance matching roughly matches the expected improvement. The representative HV longitudinal feedback signal with $f_{\text{RF}} = 1$ MHz is transmitted almost perfectly. As can be expected, the achievable signal quality decreases for higher frequency.

Figure 8 shows the first series transformer. Guanella transformer (left) and choke coil (right) are located in a housing with integrated air cooling. From long-term high-power tests, heating due to transmission line losses was identified as a limiting effect. As countermeasures, the line type was replaced by ENVIROFLEX_400 [20] and the length reduced to $l = 2.3$ m. This further increases the upper operating limit

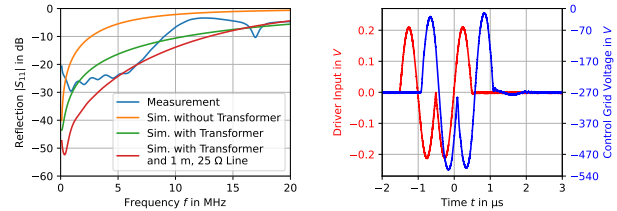
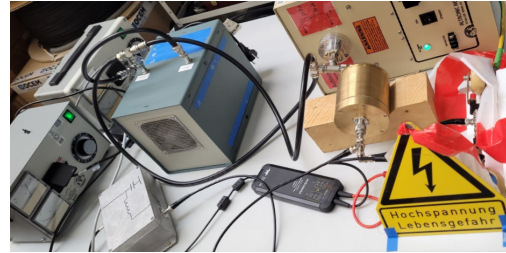


Figure 7: Measurement setup (upper picture) and results (lower diagrams) of the tetrode input circuit. Components from right to left: capacitors to emulate tetrode input capacitance (partially behind tape), high-power 12.5Ω load (box in the back), DC block, HV probe, 4:1 impedance transformer (gray box with fan), 15 mH RF filter for DC supply.

without violating the low-frequency performance requirements.

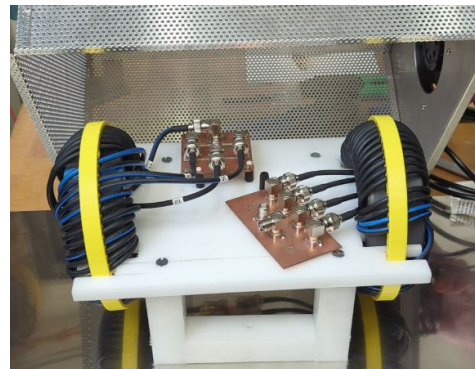


Figure 8: Series version of the 4:1 impedance transformer for the future SIS100 broadband cavities.

CONCLUSIONS

Functioning 4:1 Guanella-type broadband impedance transformers for the relevant frequency range from 100 kHz to about 15 MHz were designed, tested and verified by measurement. A compact and efficient improvement of the tetrode input circuit for the future SIS100 broadband cavities was achieved. Relevant design criteria, limitations and trade-offs were analyzed and are well understood. Further improvements of the circuit design are in progress. Applications to other problems are possible.

ACKNOWLEDGEMENTS

The authors wish to thank further members of the Ring RF department at GSI for their support of this project.

REFERENCES

- [1] P. Spiller *et al.*, “The FAIR heavy ion synchrotron SIS100,” *J. Instrum.*, vol. 15, no. 12, 2020, doi:10.1088/1748-0221/15/12/T12013
- [2] J. Schmidt *et al.*, “The SIS100 RF systems - updates and recent progress,” pp. 26–30, doi:10.18429/JACoW-IPAC2020-TUVIR14
- [3] U. Laier *et al.*, “Status and recent development of FAIR Ring RF systems,” pp. 1073–1040, doi:10.18429/JACoW-IPAC2021-MOPAB334
- [4] H. Klingbeil, U. Laier, and D. Lens, *Theoretical Foundations of Synchrotron and Storage Ring RF Systems*, 1st ed. Springer, 2016.
- [5] *R&S®BBL200 Broadband Amplifier*, Rohde & Schwarz, 2015.
- [6] *LCF12-50J - 1/2" CELLFLEX® Low-Loss Foam-Dielectric Coaxial Cable*, RFS - Radio Frequency Systems, 2022.
- [7] J. Schweickhardt, H. Klingbeil, M. Frey, K. Groß, and D. Domont-Yankulova, “Broadband nonlinear modeling of RF amplifier-driven systems for multiharmonic predistortion of pulsed output signals,” *Nucl. Instrum. Methods Phys. Res. A*, vol. 957, p. 163 433, 2020, doi:10.1016/j.nima.2020.163433
- [8] G. Guanella, “New method of impedance matching in radio-frequency circuits,” *Brown Boveri Rev.*, vol. 31, no. 9, pp. 327–329, 1944.
- [9] O. Zinke and H. Brunswig, *Hochfrequenztechnik 1: Hochfrequenzfilter, Leitungen, Antennen*, 6th ed., A. Vlcek, H. L. Hartnagel, and K. Mayer, Eds. Springer Berlin, Heidelberg, 1999, doi:10.1007/978-3-642-57131-2
- [10] H. Klingbeil, *Grundlagen der elektromagnetischen Feldtheorie*, 4th ed. Springer Spektrum Berlin, Heidelberg, 2022, doi:10.1007/978-3-662-65126-1
- [11] P. Russer, *Electromagnetics, Microwave Circuit and Antenna Design for Communications Engineering*, 2nd ed. Artech House, 2006.
- [12] D. M. Pozar, *Microwave Engineering*, 4th ed. John Wiley & Sons, 2011.
- [13] *RG316D LSFH, 50 Ohm, 6 GHz, 105°C, ø3.16 mm, RADOX® jacket - ENVIROFLEX_316_D*, HUBER+SUHNER, 2024.
- [14] J. Sevick, *Understanding, Building, and Using Baluns and Ununs*. CQ Communications, Inc., Hichsville, NY, USA, 2003.
- [15] R. W. Lewallen, “Baluns: What they do and how they do it,” *ARRL Antenna Compend.*, vol. 1, pp. 157–164, 1985.
- [16] C. J. Wegmann and H. Klingbeil, “Extended transmission line theory and its application to the broadband modeling of ferrite-based RF transformers,” *IEEE Trans. Magn.*, vol. 60, no. 12, 2024, doi:10.1109/TMAG.2024.3476925
- [17] E. Rotholz, “Transmission-line transformers,” *IEEE Trans. Microw. Theory Tech.*, vol. 29, no. 4, pp. 327–331, 1981.
- [18] C. R. Paul, *Inductance: Loop and Partial*, 1st ed. John Wiley & Sons, Inc., 2010.
- [19] *Soft Ferrites and Accessories: Data Handbook*, Ferroxcube, 2008.
- [20] *RG400 LSFH, 50 Ohm, 6 GHz, 105°C, ø5 mm, RADOX® Jacket - ENVIROFLEX_400*, HUBER+SUHNER, 2025.